nature microbiology

ARTICLES

https://doi.org/10.1038/s41564-019-0468-8

# An expanded subfamily of G-protein-coupled receptor genes in *Fusarium graminearum* required for wheat infection

Cong Jiang[1,2], Shulin Cao[1], Zeyi Wang[1], Huaijian Xu[1], Jie Liang[1], Huiquan Liu[1], Guanghui Wang[1], Mingyu Ding[1], Qinhu Wang[1], Chen Gong[1,2], Chanjing Feng[1], Chaofeng Hao[1] and Jin-Rong Xu[1,2]*

**The cAMP–PKA and MAP kinase pathways are essential for plant infection in the wheat head blight fungus *Fusarium graminearum*. To identify upstream receptors of these well-conserved signalling pathways, we systematically characterized the 105 G-protein-coupled receptor (GPCR) genes. Although none were required for vegetative growth, five GPCR genes (*GIV1*–*GIV5*) significantly upregulated during plant infection were important for virulence. The *giv1* mutant was defective in the formation of specialized infection structures known as infection cushions, which was suppressed by application of exogenous cAMP and dominant active *FST7* MEK kinase. *GIV1* was important for the stimulation of PKA and Gpmk1 MAP kinase by compounds in wheat spikelets. *GIV2* and *GIV3* were important for infectious growth after penetration. Invasive hyphae of the *giv2* mutant were defective in cell-to-cell spreading and mainly grew intercellularly in rachis tissues. Interestingly, the *GIV2*-*GIV5* genes form a phylogenetic cluster with *GIV6*, which had overlapping functions with *GIV5* during pathogenesis. Furthermore, the *GIV2*–*GIV6* cluster is part of a 22-member subfamily of GPCRs, with many of them having in planta-specific upregulation and a common promoter element; however, only three subfamily members are conserved in other fungi. Taken together, *F. graminearum* has an expanded subfamily of infection-related GPCRs for regulating various infection processes.**

The homothallic ascomycete *Fusarium graminearum* is a causal agent of head blight disease of wheat and barley and a producer of mycotoxins such as deoxynivalenol (DON)[1–3]. Ascospores are the primary inoculum that mainly infects floral tissues and certain compounds in wheat anthers appear to stimulate its virulence[4]. Under laboratory conditions, *F. graminearum* also infects floral tissues of the dicotyledonous plant *Arabidopsis*[5]. However, the underlying mechanism is not clear and the specific compounds in floral tissues recognized by this pathogen remain to be identified. In *F. graminearum*, the *Gpmk1* MAP kinase (MAPK) mutant deleted of the *PMK1* orthologue that is essential for infection structure formation and invasive growth in other fungal pathogens[6] was defective in plant infection, DON production and sexual reproduction[7,8]. The cAMP–PKA pathway and two other MAPKs, Mgv1 and FgHog1, also play critical roles in regulating mycotoxin production, ascospore formation and pathogenesis, although they have distinct roles in hyphal fusion, colonial growth and responses to hyperosmotic stress[9–12]. Although their functional relationship is not clear, the importance of these well-conserved cAMP signalling and MAPK pathways for pathogenesis and development indicates that they are coordinately involved in responses to various plant and environmental signals recognized by *F. graminearum*.

The heterotrimeric G proteins and G protein coupled receptors (GPCRs) are well conserved in fungi to activate the downstream MAPK and cAMP–PKA pathways[13]. In *F. graminearum*, the *GPA2* Gα gene is important for full virulence and DON biosynthesis[14]. Unlike animals with hundreds of GPCRs, the budding yeast has only 3 but *Neurospora crassa* has 43 GPCR genes[15,16]. In plant pathogenic fungi, GPCR genes are not well characterized although they are probably involved in fungal–plant interactions. To date, the only GPCR known to be important for plant infection is Pth11 that is involved in appressorium morphogenesis in *Magnaporthe oryzae*[17]. Pth11 has a conserved fungal-specific extracellular membrane-spanning (CFEM) domain (PF05730) that is specific for fungal GPCRs[18]. *F. graminearum* has over 100 predicted GPCR genes but only the 2 pheromone receptors have been characterized[19]. In this study, we functionally characterized all of the 105 GPCR genes and identified an expanded subfamily of infection-related GPCRs.

## Results

**None of the CFEM-containing GPCRs is essential for plant infection.** Manual annotation showed that only 105 of the 117 GPCRs predicted by automated annotation[20,21] have typical GPCR features (Supplementary Table 1). They could be divided into 8 classes[22,23], including 2 pheromone receptors[19], 1 putative carbon sensor[24], 5 cAMP receptor-like proteins and 89 Pth11-like fungal GPCRs. On the basis of RNA-seq data[25,26], 40 GPCRs had the highest expression level during infection (Supplementary Table 2). For 35 of them, the expression level was over twofold higher in infected wheat heads than in vegetative hyphae or perithecia (Fig. 1a).

Among the 89 Pth11-like GPCRs, 12 of them have typical CFEM domains[18] but only 3 of them were upregulated during wheat infection. As a result of the importance of *PTH11* in *M. oryzae*[17,18], we generated gene deletion mutants of these 12 CFEM domain-containing GPCRs. All of the resulting mutants were normal in growth and colony morphology (Supplementary Table 3). In infection assays with wheat heads, none of the mutants had significant defects in plant infection (Supplementary Fig. 1). Therefore, deletion of CFEM domain-containing GPCR genes individually had no obvious effects on pathogenesis in *F. graminearum* although

[1]State Key Laboratory of Crop Stress Biology for Arid Areas and NWAFU-Purdue Joint Research Center, College of Plant Protection, Northwest A&F University, Xianyang, China. [2]Department of Botany and Plant Pathology, Purdue University, West Lafayette, IN, USA. *e-mail: jinrong@purdue.edu

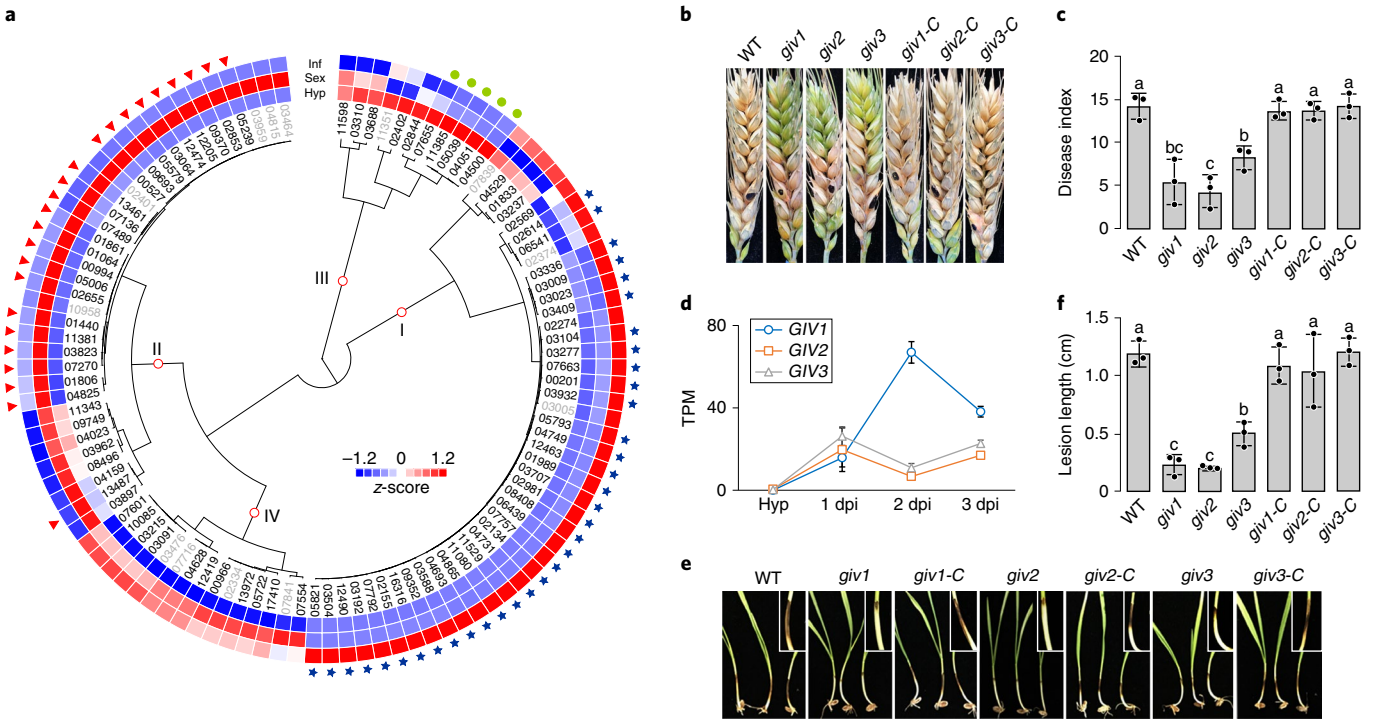


**Fig. 1 | Expression profiles of the 105 GPCR genes and mutants with defects in plant infection. a**, The 105 GPCR genes were categorized into four groups on the basis of their expression levels in vegetative hyphae (24 h yeast extract peptone dextrose (YEPD) cultures), perithecia (8 days post-fertilization (dpf)) and infected wheat heads (3 dpi). Group I, II and III GPCRs had the highest expression levels in infected wheat heads (Inf), perithecia (Sex) and vegetative hyphae (Hyp), respectively. Group IV genes were upregulated in both infected wheat heads and perithecia compared to hyphae. GPCR genes with barely detectable expression levels in all three tissues (TPM < 1) are in grey. The ones with over twofold upregulation specifically in infected wheat heads, perithecia and hyphae are labelled with blue stars, red arrowheads and green circles, respectively. **b**, Representative images of wheat heads infected with the wild type (PH-1) and the indicated *giv* mutants were photographed at 14 dpi. **c**, Mean and standard deviation of the disease index of each strain were estimated with data from three ($n = 3$) independent biological replicates (marked with black dots on the bars). Different letters indicate significant differences based on analysis of variance (ANOVA) followed by Duncan's multiple range test ($P = 0.05$). **d**, The expression levels of *GIV1*, *GIV2* and *GIV3* in vegetative hyphae (Hyp)[25] and infected wheat heads at 1, 2 and 3 dpi based on the transcripts per kilobase million (TPM) values from RNA-seq data. Mean and standard deviation were estimated with the values of three independent biological replicates ($n = 3$) presented in Supplementary Table 5. **e**, Representative images of wheat seedlings infected with the indicated *giv* mutants and complemented transformants. Insets show zoomed-in views of the diseased areas on wheat seedlings. **f**, Mean and standard deviation of the lesion length of each strain were estimated with data from at least three ($n = 3$) independent biological replicates (marked with black dots). Different letters indicate significant differences based on ANOVA analysis followed by Duncan's multiple range test ($P = 0.05$). For both **b** and **d**, similar results were obtained in three independent experiments.

it remains possible that some of them have overlapping functions during infection.

**Mutants deleted of five GPCR genes are reduced in virulence.** We then generated gene replacement mutants for the remaining 94 GPCRs (Supplementary Table 4). Whereas none of these mutants had defects in growth rate or conidium morphology and only 2 had fewer aerial hyphae or pigmentation (Supplementary Fig. 2), deletion of 13 GPCR genes resulted in over 70% reduction in conidiation (Supplementary Table 3). When assayed for mating defects, the mutants deleted of Fg05239 (a non-pheromone receptor GPCR) formed protoperithecia but failed to develop fertile melanized perithecia. Reintroducing the wild-type allele complemented its defects (Supplementary Fig. 2), confirming that Fg05239 is important for sexual development. Fg05239 orthologues are conserved in Sordariomycetes, possibly for sensing signals necessary for the further development of protoperithecia.

In infection assays with wheat heads, the vast majority of GPCR deletion mutants were normal in virulence. However, deletion of 5 GPCR genes resulted in over 25% reduction in virulence (Fig. 1b and Supplementary Table 3). All five of those *GIV* (for GPCR important for virulence) genes, Fg04693 (*GIV1*), Fg02614 (*GIV2*), Fg03104 (*GIV3*), Fg09352 (*GIV4*) and Fg02981 (*GIV5*), are Pth11-like GPCRs that were specifically expressed or significantly upregulated during plant infection (Supplementary Tables 2 and 5). In comparison with PH-1, the disease index of the *giv1* to *giv5* mutants was reduced from 25.4% to 72.5% (Fig. 1b and Supplementary Table 3) although these *giv* mutants were normal in responses to reactive oxygen species, hyperosmotic and cell wall stresses (Supplementary Fig. 3). We then selected the *giv1*, *giv2* and *giv3* mutants for complementation assays because they had more severe defects in plant infection. All of the *giv1*/*GIV1*, *giv2*/*GIV2* and *giv1*/*GIV3* complemented transformants were normal in virulence in infection assays with wheat heads (Fig. 1c,d) and coleoptiles (Fig. 1e,f), confirming the importance of these GPCR genes in pathogenesis.

***GIV1* regulates infection cushion formation and probably functions upstream of *GPA2* and the cAMP–PKA pathway.** *F. graminearum* is known to form infection cushions for plant penetration[27]. When examined by scanning electron microscopy (SEM), the *giv1* deletion mutant formed fewer and smaller infection cushions on wheat lemma than the wild-type strain PH-1 (Fig. 2a). In comparison with PH-1, the *giv1* mutant was reduced over 70% in infection cushion formation (Fig. 2b). The majority of *giv1* infection

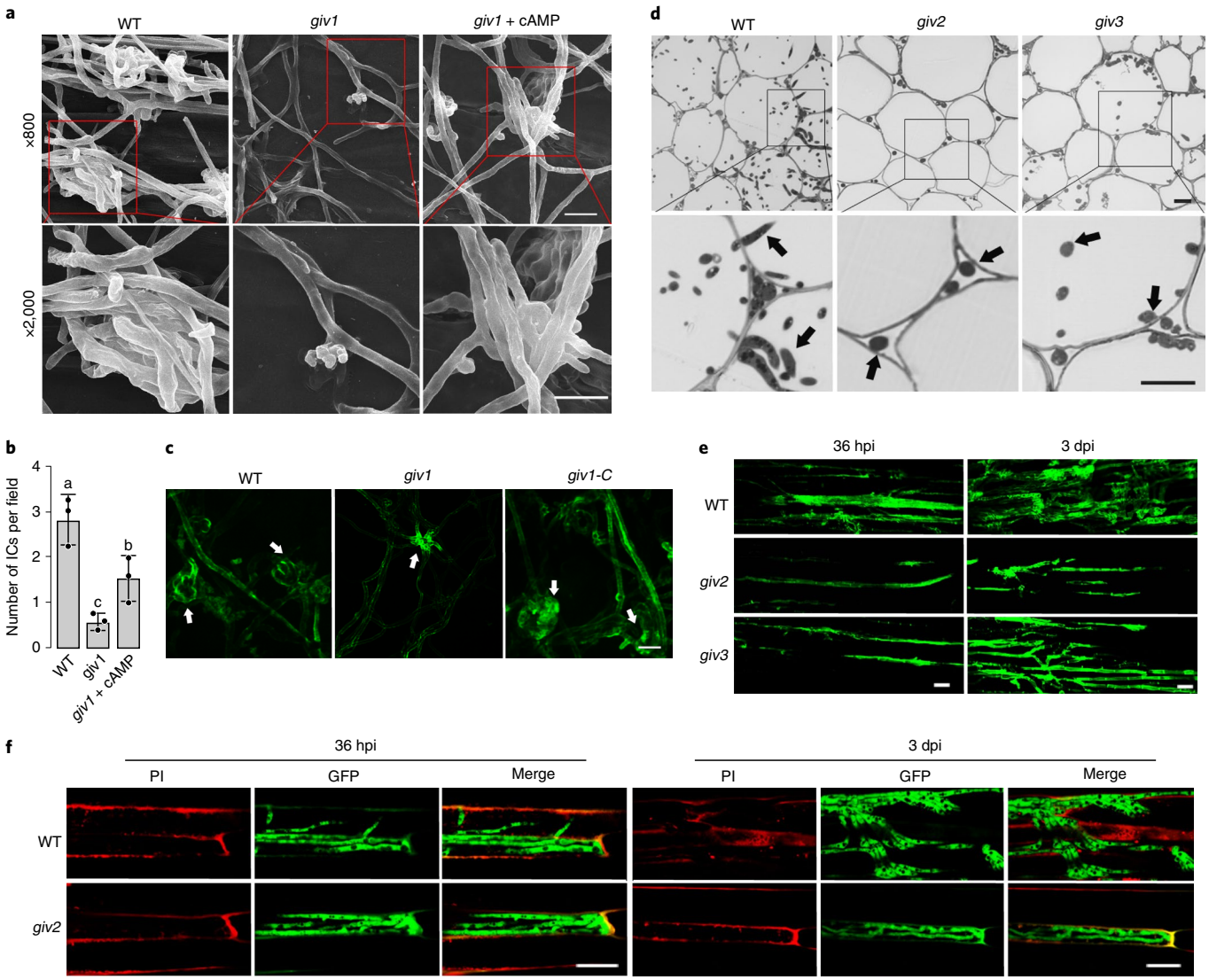


**Fig. 2 | Defects of the *giv1*, *giv2* and *giv3* mutant in infection-related morphogenesis and infectious growth. a**, Infection cushions formed by PH-1 and the *giv1* deletion mutant on wheat lemma were examined by SEM under ×800 and ×2,000 magnification at 2 dpi. Representative micrographs show the reduction in infection cushion formation (×800) and size (×2,000) in the *giv1* mutant. Scale bars, 10 μm. **b**, The average number of infection cushions (ICs) in an examination field under ×800 magnification (SEM) in lemma samples inoculated with PH-1 and the *giv1* mutant in the presence of no or 5 mM cAMP. Mean and standard deviation were estimated with data from three ($n=3$) independent replicates (marked with black dots on the bars). Different letters indicate significant differences based on ANOVA analysis followed by Duncan's multiple range test ($P=0.05$). **c**, Infection cushions formed by PH-1, the *giv1* mutant and the *giv1/GIV1* complemented strain were examined by confocal microscopy after staining with Alexa Fluor 488. The arrows point to infection cushions. Scale bar, 20 μm. **d**, Thick sections of the rachises of wheat heads inoculated with the same set of strains were examined for invasive hyphae at 5 dpi. Infected tissues were embedded in Spurr resin after fixation with 3% glutaraldehyde and dehydration in graded series of 30–100% of ethanol before being sectioned. The lower panels are zoom-in views of the framed areas to show the defects of *giv2* and *giv3* mutants in infectious growth. The arrows point to intracellular or intercellular invasive hyphae. Scale bars, 20 μm. For **a**–**d**, similar results were obtained in three independent experiments. **e**, Wheat seedlings inoculated with transformants of the wild-type, *giv2* and *giv3* mutant strains expressing cytoplasmic GFP were examined for infectious growth by epifluorescence microscopy at 36 hpi and 3 dpi. Scale bars, 20 μm. **f**, Invasive hyphae formed by transformants of PH-1 and the *giv2* mutant expressing cytoplasmic GFP in infected coleoptile cells at 36 hpi or 3 dpi were examined after staining the plant cell wall with propidium iodide (PI), which binds to demethoxylated pectins. Scale bars, 20 μm. For **e** and **f**, similar results were obtained in six independent experiments.

cushions were less complex and had limited branches. Confocal microscopy examination after staining with Alexa Fluor 488[28] also showed that the *giv1* mutant was reduced in the number and size of infection cushions formed on wheat lemma (Fig. 2c).

To determine the relationship between Giv1 and Gpa2, the major Gα subunit for pathogenesis[14], we first generated the *GPA2*–GFP and $P_{RP27}$-*GIV1*–3×FLAG constructs and transformed them into PH-1. Transformants expressing both fusion constructs were identified by PCR and confirmed by western blot analysis (Supplementary Fig. 4). In total proteins isolated from vegetative hyphae of the *GPA2*–GFP *GIV1*–3×FLAG transformant and proteins co-purified with anti-FLAG M2-agarose beads, the 67-kDa Gpa2–GFP band could be detected with an anti-GFP antibody (Supplementary Fig. 5), indicating their direct interaction in vivo. We also generated transformants of *giv1* expressing the dominant active $GPA2^{DA}$ allele. In comparison with *giv1*, the *giv1*/$GPA2^{DA}$ transformants formed more

and larger infection cushions, although not as many as the wild type (Supplementary Fig. 5), but were still defective in plant infection, which is consistent with the defects of *GPA2*$^{DA}$ transformants in pathogenesis as previously reported[29], indicating that expressing *GPA2*$^{DA}$ partially rescues the defects of the *giv1* mutant.

Exogenous 5 mM cAMP also significantly increased infection cushion formation in the *giv1* mutant (Fig. 2b) although not to the wild-type level. Treatment with 2.5 mM 3-isobutyl-1-methylxanthine (IBMX), an inhibitor of cAMP phosphodiesterase, had similar effects in stimulating infection cushion formation in the *giv1* mutant (Supplementary Fig. 6). In addition, the *cpk1 cpk2* mutant[9], similar to the *giv1* mutant, was defective in infection cushion formation (Supplementary Fig. 6). These results suggest that cAMP treatment or overstimulating PKA partially suppresses the *giv1* mutant defects in the development of infection cushions. *GIV1* may function upstream from the cAMP–PKA pathway in *F. graminearum* for regulating infection cushion formation.

***GIV2* and *GIV3* are important for infectious growth.** Unlike the *giv1* mutant, the *giv2* and *giv3* mutants had no obvious defects in infection cushion formation (Supplementary Fig. 7). By 48 h post-inoculation (hpi), invasive hyphae were frequently observed in lemma tissues of samples inoculated with the wild type and *giv2* or *giv3* mutant (Supplementary Fig. 8), suggesting that deletion of *GIV2* or *GIV3* had no obvious effects on the initial plant penetration and development of infectious hyphae. When examined for infectious growth in the rachis, which is essential for the pathogen spreading in wheat heads[30], abundant invasive hyphae were observed in samples inoculated with PH-1 at 5 days post-inoculation (dpi; Fig. 2d) and the *giv2*/*GIV2* and *giv3*/*GIV3* complementation transformants (Supplementary Fig. 8). Under the same conditions, fewer hyphae were observed in rachis tissues above or below the infected spikelet inoculated with the *giv2* or *giv3* mutant, particularly in the *giv2* samples (Fig. 2d). In repeated assays, extensive hyphal growth to the wild-type level was not observed in the rachis tissues of *giv2*- or *giv3*-infected wheat heads. For the *giv2* mutant, invasive hyphae often grew in the intercellular spaces in infected tissues, probably due to its defects in penetrating neighbouring plant cells. These results indicate that *GIV2* and *GIV3*, particularly *GIV2*, play important roles in the colonization of rachis tissues and spreading via the rachis.

We also examined invasive hyphae formed by transformants of the *giv2* and *giv3* mutants expressing cytoplasmic GFP in wheat coleoptile cells as described previously[31]. The *giv2* and *giv3* mutants were able to colonize through wounds and developed invasive hyphae. However, in comparison with PH-1, spreading of invasive hyphae was less extensive in the *giv2* and *giv3* mutants, particularly in *giv2* (Fig. 2e). To confirm the importance of *GIV2* in the cell-to-cell movement and spreading of invasive hyphae, we stained plant cell walls with propidium iodide[32]. In samples inoculated with the *giv2* mutant, invasive hyphae were often restricted to the initial penetrated coleoptile cells at 36 hpi (Fig. 2f). Even at 3 dpi, invasive hyphae of *giv2* still had limited growth and rarely spread transversely to neighbouring coleoptile cells (Fig. 2f).

***GIV1* may be involved in sensing floral tissue factors.** To use the similar chemotropic growth assay developed in *Fusarium oxysporum*[33], we first deleted the *ROA* gene in the wild type and *giv* mutants to generate *roa* mutants that produce mainly unicellular ascospores[34]. In chemotropic sensing and germ tube growth assays, ascospores of the resulting *roa* mutants had similar responses to glucose, glutamine, aspartic acid, glycerol and galactose (Supplementary Fig. 9). As flowering wheat heads are known to stimulate the virulence of *F. graminearum*[4], we then assayed the effects of the water, ethyl acetate and chloroform extracts of flowering spikelets on chemotropic growth of germ tubes. Unlike treatments with the water and ethyl acetate extracts, the chloroform extract affected the direction of germ tubes in the *roa* mutant (Fig. 3a). We then treated ascospores of the *giv1 roa*, *giv2 roa* and *giv3 roa* double mutants with the chloroform extract. Whereas the *giv2 roa* and *giv3 roa* mutants were similar to the *roa GIV*$^{WT}$ mutant in chemotropic growth, *giv1 roa* ascospores were defective in response to the chloroform extract (Fig. 3b). These results suggest that deletion of *GIV1*, but not *GIV2* or *GIV3*, affects chemotropic sensing of wheat spikelet compounds.

We then isolated proteins from hyphae treated with flowering spikelets as described in the Methods and assayed for PKA activities[35]. In the wild type, treatments with wheat spikelets significantly stimulated PKA activities. However, the stimulatory effects of wheat spikelets on PKA activities were reduced in the *giv1* and *giv3* mutants (Fig. 3c,d and Supplementary Fig. 10). Treatments with wheat spikelets also increased the intracellular cAMP level significantly more in the wild type than in the *giv1* mutant (Supplementary Fig. 11). These results indicate that *GIV1*, and possibly *GIV3*, may be involved in sensing spikelet compounds to activate the cAMP–PKA pathway.

**Giv1 functions upstream from the Gpmk1 pathway.** Treatments with wheat spikelets also stimulated the phosphorylation of both Gpmk1 and Mgv1 in the wild type (Fig. 3e,f and Supplementary Fig. 12) but had no effects on the activation of FgHog1 (Supplementary Fig. 13). Whereas deletion of *GIV2* and *GIV3* had no significant effects, the *giv1* mutant was significantly reduced in the stimulation of Gpmk1 phosphorylation by wheat spikelets (Fig. 3e,f). These results suggest that certain spikelet compounds are recognized by *F. graminearum* to activate Gpmk1, probably involving Giv1 and other GPCRs. To test this hypothesis, we generated the dominant active allele of *FST7* that encodes the MEK kinase activating Gpmk1[36,37]. In comparison with the *giv1* mutant, *giv1*/*FST7*$^{DA}$ transformants were increased in infection cushion formation on wheat lemma (Fig. 4a). In infection assays with wheat heads, expression of *FST7*$^{DA}$ also partially rescued the defects of the *giv1* mutant in virulence (Fig. 4b,c), further indicating that Giv1 is one of the GPCRs functioning upstream from Gpmk1.

On activation, some MAPKs are translocated into the nucleus to phosphorylate their downstream targets[38,39]. Treatments with wheat spikelets also had a stimulatory effect on the nuclear localization of Gpmk1 (Fig. 4d). In the Gpmk1–GFP transformant of the wild type, approximately 50% of the nuclei in germ tubes had clear GFP signals in the nucleus in comparison with the cytoplasmic background. In the germ tubes of the *giv1* Gpmk1–GFP transformants, only 25% of the nuclei had clear GFP signals (Fig. 4e). Therefore, *GIV1* may be involved in sensing spikelet compounds for the activation and translocation of Gpmk1 into the nucleus.

**Expansion of the *GIV* cluster and a subfamily of infection-related GPCRs.** Phylogenetic analysis showed that although none of them was essential for plant infection, the 12 CFEM-domain containing GPCRs are in 1 clade (Fig. 5a). Interestingly, four of the five *GIV* genes (Giv2–Giv5) form a small cluster with Fg05793 (named *GIV6* below). Furthermore, all of the members of the *GIV* cluster were upregulated over tenfold or specifically expressed during plant infection (Supplementary Fig. 14). The *GIV2*–*GIV6* genes are closely related to 17 other GPCRs (Fig. 5a) with similar structural components (Supplementary Fig. 15). In total, 11 members of this GPCR subfamily (named EIG, for expanded infection-related GPCR genes below) had a greater than tenfold increase in expression levels or were almost specifically expressed in infected wheat heads (Fig. 5b). Another two members of this subfamily had over eightfold and threefold in planta-specific upregulation. Comparative analysis with *M. oryzae* and *N. crassa* showed that 13 of the 22 GPCRs in this EIG subfamily are unique to *F. graminearum*. Among the rest, six have homologues in *M. oryzae* but not in *N.* crassa. Only *GIV5*

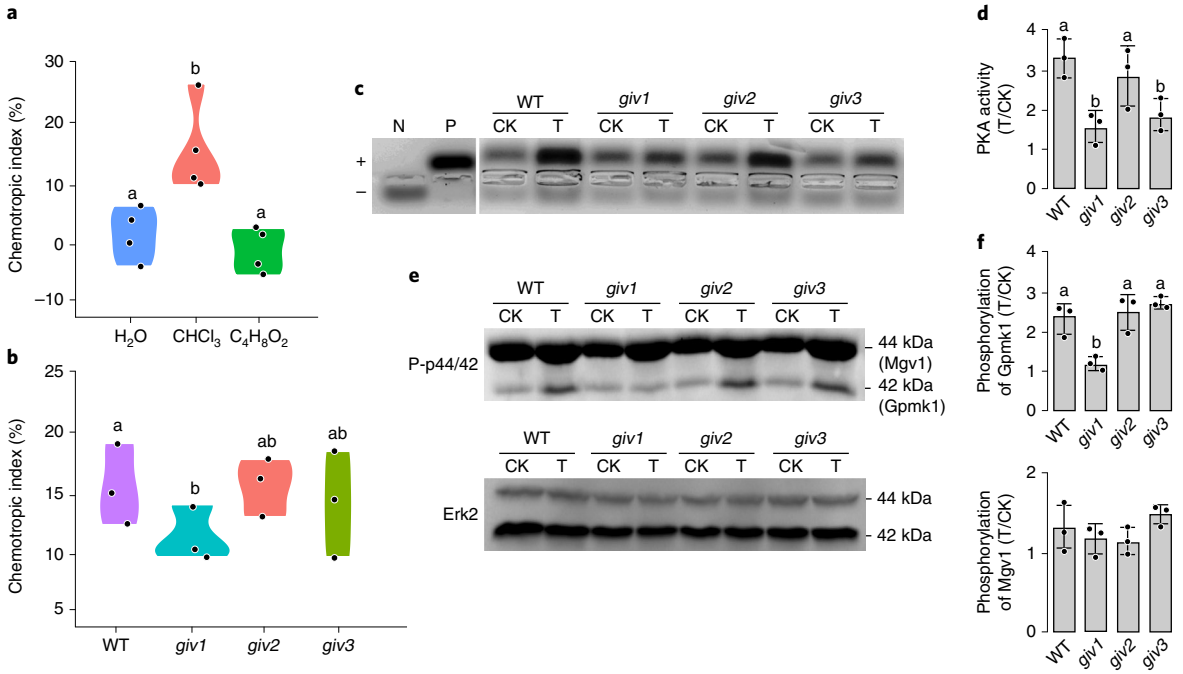


**Fig. 3 | Assays for the effects of wheat spikelets on PKA activities and activation of MAPKs. a**, Violin plots of the chemotropic index of the *roa* mutant treated with the water, chloroform or ethyl acetate extract of wheat spikelets were generated with the R program. **b**, Violin plots of the chemotropic index of the *roa giv1, roa giv2* and *roa giv3* double mutants treated with the chloroform extract of wheat spikelets. For **a** and **b**, the coloured density region shows the distribution shape of the chemotropic index data calculated as $(H_{test}-H_{solv})/H_{total}\times100$. $H_{test}$ and $H_{solv}$ were the number of germ tubes that grew towards the test compound and solvent control, respectively. Each dot on the violin plots represents the chemotropic index of an individual biological replicate ($n=4$ for **a**; $n=3$ for **b**) with at least 100 germ tubes examined in each replicate. **c**, Proteins extracted from hyphae of the marked strains treated with (T) or without wheat spikelets (CK) were assayed for PKA activities with the PepTag non-radioactive PKA assay kit. Positive and negative controls are from the kit. '+' and '−' indicate the anode and cathode, respectively. **d**, Band densities were analysed with Image Lab Software to estimate changes in PKA activities in the marked strains when treated with wheat spikelets in comparison with untreated samples. **e**, Representative western blots of proteins isolated from hyphae of the wild type and indicated mutants treated with (T) or without (CK) of wheat spikelets were assayed for the expression and activation of Gpmk1 (42 kDa) and Mgv1 (44 kDa) with the anti-MAPK and anti-TpEY antibodies, respectively. Detection with the anti-Erk2 antibody showed similar expression levels of Gpmk1 and Mgv1 in all of the samples. **f**, The densities of the Gpmk1 and Mgv1 bands were analysed with Image Lab Software to estimate changes in their phosphorylation levels in hyphae treated with wheat spikelets. In **d** and **f**, the mean and standard deviation of the ratio between treated and untreated (arbitrarily set to 1) samples were estimated with data from three ($n=3$) independent replicates (marked with black dots). Different letters indicate significant differences based on ANOVA analysis followed by Duncan's multiple range test ($P=0.05$) in **a**,**b**,**d**,**f**.

and two other GPCR genes are common to all three fungal species (Fig. 5b). These data suggest that GPCRs in the EIG subfamily have been expanded in plant pathogenic fungi, particularly in *F. graminearum*. Furthermore, 19 of the 22 EIG GPCR genes are in the fast-evolving genomic regions[40], including two of them, Fg13461 and Fg11529, that are near the telomeric regions (Supplementary Fig. 16). Therefore, most members of this expanded GPCR family may be under positive selection for infection-related functions.

Interestingly, 10 of the 13 EIG GPCRs with upregulated expression during infection have a putative promoter element (PPE) with the RRMCAACA consensus sequence (Fig. 5c). This PPE sequence is also present in 17 of 22 other non-EIG GPCRs with over two-fold in planta-specific upregulation (Supplementary Fig. 17) but only in 6 of the 29 GPCRs specifically upregulated in perithecia or hyphae. Therefore, this PPE is significantly enriched in GPCRs with in planta-specific upregulation. To characterize its function in regulating Fg07792, a GPCR specifically expressed in infected wheat heads, Fg07792–GFP fusion constructs under the control of its native promoter (PPE$^+$) or a promoter deleted of this sequence (ΔPPE) were transformed into the Fg07792 deletion mutant. In the resulting transformants, the expression of the transforming PPE$^+$ construct was increased over 100-fold in infected wheat heads compared to vegetative hyphae. The ΔPPE construct also had increased expression during plant infection but its increase was less than 5.5-fold (Fig. 5d). In similar experiments with *GIV5*, whereas the PPE$^+$ transformants had over a 30-fold increase in its expression during plant infection, the upregulation of *GIV5* expression in infected wheat heads was significantly diminished in the ΔPPE transformant (Supplementary Fig. 18). These results indicated that this promoter element is important for the upregulation of Fg07792 and *GIV5* during plant infection. Some of the seven transcription factors identified by systemic characterization in *F. graminearum* to play stage-specific roles during plant infection[41] may be involved in the co-regulation of these infection-related GPCRs via the PPE sequence.

To test whether members of the EIG subfamily have overlapping functions, we generated Fg07757 Fg04749 and *giv5 giv6* (Fg05793) double mutants on the basis of their close phylogenetic relationship and similar expression profiles (Fig. 5b). The Fg07757 Fg04749 double mutants, similar to the Fg07757 or Fg04749 mutant, had no obvious defects in vegetative growth and plant infection (Supplementary Fig. 19). The *giv5 giv6* double mutant was also normal in vegetative growth but it had more severe defects in virulence (Fig. 5e) and infectious growth (Fig. 5f) than the *giv5* mutant. Therefore, *GIV5* and *GIV6* probably have overlapping functions in sensing host factors and regulating infectious growth.

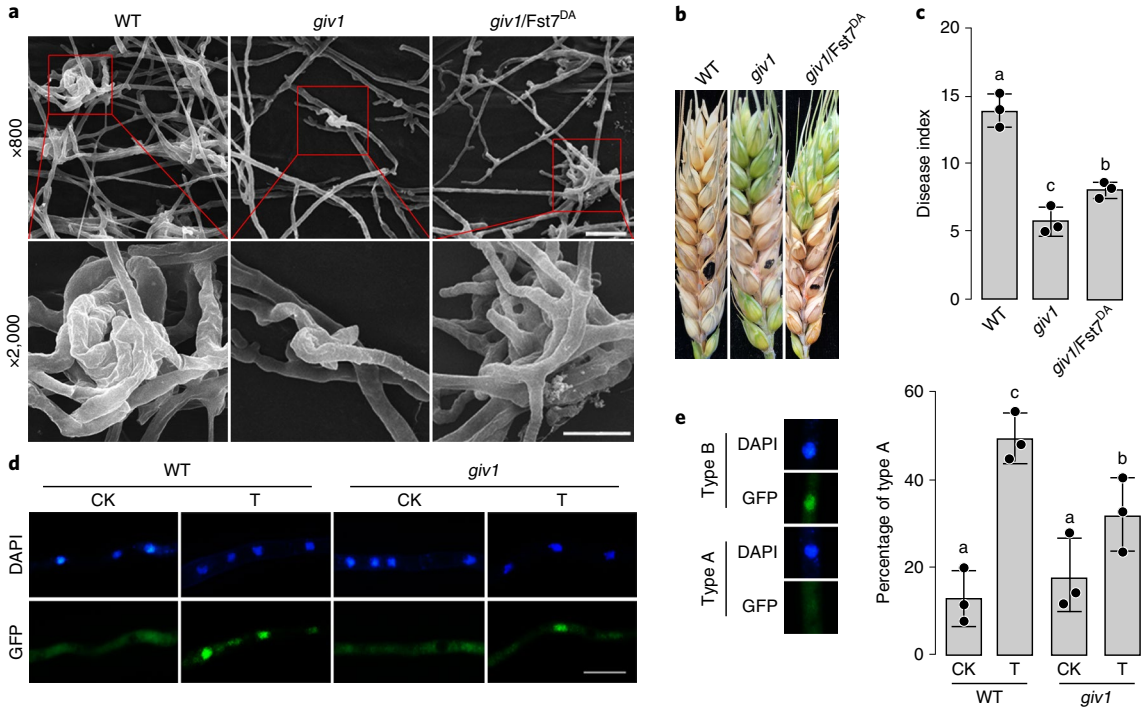


**Fig. 4 | Assays for the effects of dominant active *FST7* and nuclear localization of Gpmk1–GFP. a**, Formation of infection cushions on lemma by the *giv1* mutant and the *giv1 FST7*$^{DA}$ transformant expressing cytoplasmic GFP. Scale bars, 10 μm. Similar results were obtained in three independent experiments. **b**, Representative images of wheat heads infected with the wild type (PH-1), *giv1* mutant and *giv1/FST7*$^{DA}$ transformant were photographed at 14 dpi. **c**, The mean and standard deviation of the disease index of each strain were estimated with data from three independent replicates (marked with black dots on the bars). Different letters indicate significant differences based on ANOVA analysis followed by Duncan's multiple range test ($P = 0.05$). **d**, Germlings of transformants of PH-1 and the *giv1* mutant expressing the Gpmk1–GFP fusion treated with (T) or without (CK) wheat spikelets for 30 min were stained with 4′,6-diamidino-2-phenylindole (DAPI) and counted for the percentage of nuclei with GFP signals in the nucleus that were above the cytoplasm background (type A). For type B nuclei, GFP signals in the nucleus were similar to that of the cytoplasm background. Scale bar, 10 μm. **e**, The mean and standard deviation of the percentage of type A nuclei were estimated with data from three ($n = 3$) independent replicates (marked with black dots on the bars). Different letters indicate significant differences based on ANOVA analysis followed by Duncan's multiple range test ($P = 0.05$).

## Discussion

GPCRs are the largest class of cell-surface receptors in fungi that lack receptor or receptor-like kinases. *F. graminearum* has 105 GPCRs, which is more than the 43 in *N. crassa* and 61 in *M. oryzae*[42]. The expansion of EIG genes in *F. graminearum* and their specific or upregulated expression during infection suggest that these GPCRs may play roles in pathogenesis, which is supported by the functions of the *GIV* genes. Furthermore, 19 of the 22 EIG GPCRs are in the fast-evolving subgenome enriched for genes involved in fungal–plant interactions[40]. Therefore, members of this expanded GPCR subfamily may be under positive selection for sensing host and environmental signals during disease development.

The *giv1* mutant was defective in infection cushion formation on plant surfaces and response to the chloroform extract of flowering spikelets for germ tube growth. Although it is not clear what spikelet compounds were extracted by chloroform, chloroform is more suitable than ethyl acetate for the extraction of less polar compounds and will preferentially remove the waxy surface layers of the spikelet. Our data showed that Giv1 may function upstream from both the cAMP–PKA and Gpmk1 MAPK pathways. As in *M. oryzae* and other plant pathogens[6,43], both the cAMP-signalling and Gpmk1 pathways are important for pathogenesis and differentiation in *F. graminearum*[10]. Although the exact relationship between these two pathways is not clear, they must crosstalk and coordinate to regulate responses to different signals recognized by Giv1 and other GPCRs at different stages.

As the only *GIV* gene not in the EIG subfamily, *GIV1* forms a small cluster with three other GPCR genes (Fig. 5a) that may have overlapping functions in recognizing plant surface signals because the *giv1* mutant was reduced but not blocked in infection cushion formation. Interestingly, *GIV1* is conserved in *M. oryzae*, which forms appressoria on leaves and hyphopodia on roots for plant penetration. As infection cushions formed by *F. graminearum* are more similar to hyphopodia, it is possible that the *GIV1* orthologue is involved in regulating hyphopodium formation in *M. oryzae*[23].

Giv2 may be important for recognizing host signals for cell-to-cell penetration and spreading of invasive hyphae in infected plant tissues. Recently, both Mgv1 and Pmk1 MAPKs have been shown to regulate the cell-to-cell spreading of invasive hyphae in *M. oryzae*[44,45]. In *F. graminearum*, Giv2 may function upstream from these conserved MAPK cascades to regulate infectious growth. Giv3 is also important for infectious growth and the *giv3* mutant was reduced in PKA activities. *GIV3*, like other members of the EIG subfamily, had over tenfold in planta-specific upregulation. Some of these EIG GPCRs may have overlapping functions during plant infection and it will be important to generate and characterize mutants deleted of two or multiple EIG genes with similar sequences and expression profiles. Ultimately, it will be important to identify the plant factors or ligands recognized by different GPCRs at various infection stages.

## Methods

**Bioinformatics analysis with GPCR genes.** The predicted gene models of all the putative GPCR genes[21] were exacted from the genome annotation of *F. graminearum* PH-1 (V3, downloaded from the Broad Institute) and manually annotated on the basis of published RNA-seq data of vegetative hyphae from YEPD cultures and perithecia (8 dpf) (NCBI SRA database accession number SRP062731)[25] and RNA-seq data of infected wheat heads generated in this study.

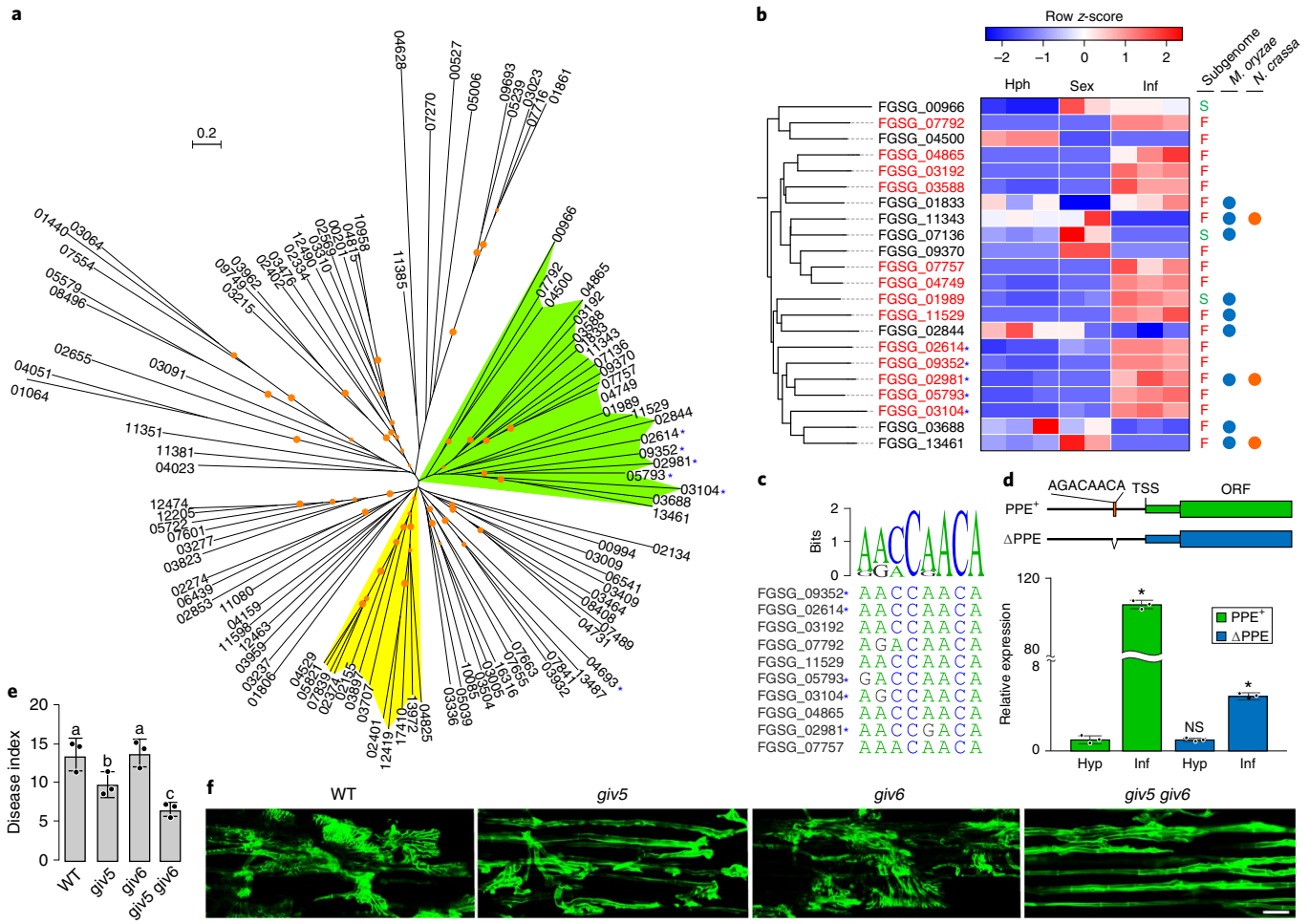


**Fig. 5 | GPCR genes of the EIG subfamily. a**, A phylogenetic tree of 105 GPCR genes constructed by the maximum-likelihood method using PhyML3.1. The orange circles mark the branches with Shimodaira–Hasegawa-like support of approximate likelihood ratios (aLRT-SH) larger than 0.5. The EIG and CFEM clusters are shaded in green and yellow, respectively. *GIV* genes are marked by an asterisk. **b**, The phylogenetic relationship, expression profiles and chromosomal distribution of EIG genes and their homologues in *M. oryzae* and *N. crassa*. The GPCR genes with over twofold specific upregulation in infected wheat heads are in red. F, fast genome; S, slow genome. **c**, A common promoter element identified in the promoter regions of ten EIG genes specifically upregulated during plant infection. **d**, Relative expression levels of Fg07792 in transformants of its deletion mutant expressing the PPE$^+$ (intact promoter) and ΔPPE (deleted of AGACAACA) constructs were assayed by quantitative PCR with reverse transcription (qRT-PCR) with RNA isolated from vegetative hyphae (Hyp) and infected wheat heads sampled at 3 dpi (Inf). TSS, transcription start site. The ubiquitin carboxy-terminal hydrolase gene (*GzUBH*) was used as the internal control. The mean and standard deviation of the relative expression level of Fg07792 were estimated with results from three ($n=3$) independent biological replicates. Each dot on the bars represents the value of individual replicates. The asterisk indicates significant differences ($P=0.0005$) based on Bootstrap analysis by BootstRatio. NS, not significant. **e**, The mean and standard deviation of the disease index scored on infected wheat heads were estimated with data from three ($n=3$) independent replicates (marked with black dots) for the marked strains. Different letters indicate significant differences based on ANOVA analysis followed by Duncan's multiple range test ($P=0.05$). The *giv5 giv6* double mutant had more severe defects in wheat head infection than the *giv5* and *giv6* single mutants. **f**, Invasive hyphae formed by PH-1 and labelled mutants expressing cytoplasmic GFP in wheat coleoptile cells at 3 dpi. The *giv5 giv6* mutant had more severe defects than the *giv5* mutant in infectious growth. Scale bar, 20 μm. Similar results were obtained in six independent experiments.

A total of 18 putative GPCR genes were revised due to errors in automated annotation (Supplementary Table 1). The corrected sequences of these 18 genes have been deposited in GenBank under accession numbers MK510897–MK520914. All of the amino-acid sequences of GPCRs were then analysed for transmembrane helices by TMHMM 2.0 and TOPCONS. Twelve of them were found to lack typical GPCR features (Supplementary Table 1), including ten with fewer than seven transmembrane helices.

The 105 GPCR genes could be divided into different groups based on RNA-seq data of infected wheat heads (3 days dpi), vegetative hyphae from YEPD cultures and perithecia (8 dpf)[25]. Among the 40 group I GPCRs with the highest expression level during infection, the expression levels of 35 of them were over twofold higher in infected wheat heads than in vegetative hyphae or perithecia. Whereas 24 of the group II genes had over twofold higher expression levels in perithecia, only 5 of the group III GPCRs were upregulated over twofold in vegetative hyphae compared to the other 2 stages. The expression of 15 group IV GPCRs was increased in both infected wheat heads and perithecia compared to hyphae. Multiple sequence alignments of GPCR proteins were generated with the M-Coffee program. Phylogenetic trees were constructed using MEGA with the neighbour-joining method and further visualized using the ITOL tool. Heat maps of expression values were drawn with the heatmap function in R (www.r-project.org). The 1 kilobase sequences upstream from the transcription start site of all the GPCR genes were extracted and analysed with the MEME Suite for common promoter elements.

**Strains and culture conditions.** The wild-type *F. graminearum* strain PH-1 (ref. [21]) and deletion mutants of GPCR genes were routinely cultured on potato dextrose agar (PDA) plates at 25 °C. The growth rate on PDA plates and conidiation in liquid carboxymethyl cellulose (CMC) medium were assayed as previously described[12,37]. The final concentration of 0.5 mM $H_2O_2$, 0.7 M NaCl

or 150 μg ml$^{-1}$ Congo red was added to PDA for assaying stress responses[37]. Protoplast preparation and PEG-mediated transformation were performed as described previously[12]. For selection of transformants, hygromycin B and geneticin (Calbiochem) were added to the final concentration of 300 and 200 μg ml$^{-1}$, respectively, to the top agar. Mating and perithecium formation were assayed on carrot agar plates as described previously[37].

**Generation of gene deletion mutants and complementation strains.** All of the gene replacement constructs were generated with the split-marker approach[37]. The flanking sequences of individual GPCRs were amplified and connected to the hygromycin phosphotransferase (*hph*) cassette by overlapping PCR with the primers listed in Supplementary Table 6. The resulting PCR products were transformed into PH-1 and gene replacement mutants were identified by PCR with the primers listed in Supplementary Table 6. For each GPCR gene, at least two independent gene replacement mutants (Supplementary Table 4) were identified by PCR assays (Supplementary Figs. 20 and 21). To generate the *giv5 giv6* mutants, the flanking sequences of *GIV5* were amplified and connected to the geneticin-resistance marker amplified from pFL2[46] and transformed into the *giv6* mutant. Transformants resistant to both hygromycin and geneticin were screened by PCR for double mutants. Similar approaches were used to generate the Fg07757 Fg04749 deletion mutants (Supplementary Fig. 21).

For complementation assays, the entire *GIV1* gene with its native promoter was cloned into pFL2 by gap repair[38,46] and transformed into the *giv1* mutant. The *giv1*/*GIV1* transformants were identified by PCR and assayed for phenotype complementation. The same approach was used for complementation assays with the *giv2*, *giv3* and Fg05239 deletion mutants.

**Generation of *GPA2*$^{DA}$, *FST7*$^{DA}$ and *GPMK1*–GFP transformants.** The S216D T220E amino-acid changes[36,47] were introduced into *FST7* by overlapping PCR with primers carrying the corresponding mutations. The resulting PCR products were cloned into vector pFL2 as described to generate the *FST7*$^{DA}$ construct. After verification by sequencing analysis, *FST7*$^{DA}$ was transformed into PH-1 and the *giv1* mutant. The dominant active allele of *GPA2* was generated by introducing the Q207L mutation as described previously[29]. The resulting *GPA2*$^{DA}$ construct was verified by sequencing analysis and transformed into the *giv1* mutant. The *GPMK1*–GFP fusion construct was generated by cloning *GPMK1* into pFL2[46] and transformed into PH-1 and *giv1* mutant. *GPMK1*–GFP transformants were identified by PCR and examined by epifluorescence microscopy. To assay changes in its subcellular localization, germlings collected from 18 h YEPD cultures were treated with or without wheat spikelets for 30 min. After staining with DAPI, the percentage of nuclei in germ tubes with clear GFP signals in the nucleus (above the cytoplasm background) was counted. Data from 3 independent replicates, with 60 germ tubes (over 200 nuclei examined) per replicate, were analysed by ANOVA analysis followed by Duncan's multiple range test ($P = 0.05$).

**Infection assays with flowering wheat heads.** Conidia of PH-1 and mutant strains freshly collected from 5-day-old CMC cultures were resuspended to $10^5$ spores ml$^{-1}$ in sterile double-distilled water (DDW). Flowering wheat heads of 6-week-old wheat cultivar XiaoYan 22 (ref. [48]) plants were inoculated with 10 μl of conidium suspensions at the fifth spikelet from the base. XiaoYan 22 is a winter wheat cultivar selected for its yield and grain quality in a breeding program at Northwest A&F University in China[49] but it is fully susceptible to *F. graminearum* infection[48]. Spikelets with typical wheat scab symptoms were examined at 14 dpi to estimate the disease index[50]. The mean and standard deviation of the disease index were estimated with data from three independent replicates with at least ten wheat heads examined in each replicate. For assaying infectious growth, infected lemma and rachis tissues were embedded in Spurr resin after fixation and dehydration as described previously[9,48]. Thick sections were then prepared and stained with 0.5% (wt/vol) toluidine blue and examined with an Olympus BX-53 microscope.

**Assays for infection cushion formation.** Intact flowering wheat heads of 6-week-old wheat cultivar XiaoYan 22 (ref. [48]) plants grown under a 15/9 h light/dark period were inoculated with conidium suspensions ($2 \times 10^4$ spores ml$^{-1}$ in DDW) as described previously[12,51]. Inoculated wheat heads were capped with a plastic bag for 48 h to retain the moisture. After removing the plastic bags, lemmas were collected and fixed with 4% (vol/vol) glutaraldehyde in 0.1 M phosphate buffer (pH 6.8) overnight at 4 °C. After dehydration in a series of acetone, the samples were coated with gold–palladium and examined with a JEOL 6360 scanning electron microscope (Jeol) as described previously[51]. For each strain, at least five different lemmas were examined for infection cushions in each independent experiment. Inoculated lemmas were also stained with Alexa Fluor 488 and examined by epifluorescence microscopy as described previously[28]. To determine their effects on infection cushion formation, cAMP and IBMX were added to the final concentration of 5 mM and 2.5 mM, respectively, to spore suspensions before inoculation.

**Infection assays with wheat seedlings.** Three-day-old seedlings of the wheat cultivar Norm were used for infection assays as described previously[31]. Briefly, the top 1–2 mm portion of wheat coleoptiles was excised and inoculated with 2 μl of freshly prepared conidium suspensions ($10^5$ spores ml$^{-1}$) over the wound sites. The seedlings were then grown at 25 °C with a 12 h light/12 h dark photoperiod. Necrotic lesions on leaf sheaths were measured at 10 dpi. For examining invasive hyphae by confocal microscopy, the $P_{RP27}$-GFP construct was transformed into the wild type and *giv* mutants. Wheat coleoptiles inoculated with transformants with GFP signals in the cytoplasm were sampled at 36 or 72 hpi and examined with a Nikon A1 confocal microscope.

**Assays for PKA activity and intracellular cAMP levels.** Vegetative hyphae were collected by filtration after culturing $10^8$ conidia in 100 ml YEPD for 12 h. After washing with DDW and dividing into halves, each half was resuspended in 20 ml DDW with or without 8 dissected-apart flowering spikelets of 6-week-old wheat cultivar XiaoYan 22 plants that had the anthers in approximately a third of the florets exposed. After incubation for 1 h at 25 °C, spikelets were removed and hyphae were collected by filtration and used for protein extraction as described previously[35]. PKA activities were assayed with the PepTag non-radioactive PKA assay kit (Promega) by detecting the phosphorylation of PegTagA1 peptide-LRRASLG as described previously[52]. The cAMP Biotrak Immuno-assay System (Amersham Biosciences) was used to assay the intracellular cAMP levels in hyphae treated with or without wheat spikelets as described above and in hyphae collected from 3-day-old CMC cultures[53].

**MAPK phosphorylation assays.** Vegetative hyphae were collected from 12 h YEPD cultures and treated with wheat spikelets as described above for PKA activity assays. Total proteins were isolated from vegetative hyphae with protein lysis buffer containing protease inhibitor cocktail (cat. no. P8340, Sigma-Aldrich) and phosphatase inhibitor cocktails 2 (cat. no. P0044, Sigma-Aldrich) and 3 (cat. no. P5726, Sigma-Aldrich) as described previously[54]. Expression and phosphorylation of Gpmk1 or Mgv1 were detected with an anti-Erk2 antibody (Santa Cruz Biotechnology) and the PhosphoPlus p44/42 MAPK antibody kit (Cell Signaling Technology) as described previously[54]. Phosphorylation of FgHog1 was assayed with the Phospho p38 MAPK antibody kit (Cell Signaling Technology). The specificities of anti-TpEY and anti-TpGY antibodies were verified (Supplementary Fig. 23) with the *gpmk1*, *mgv1* and *Fghog1* deletion mutants[45,55]. Band densities were analysed with the Image Lab software. Quantitative changes in the phosphorylation levels of Gpmk1 and Mgv1 were analysed with the Image Lab software. For the Mgv1 MAPK, treatments with spikelets stimulated its phosphorylation in the wild type and all three *giv* mutants to various degrees (Fig. 3e,f and Supplementary Fig. 12). Unlike Gpmk1 and Mgv1, treatments with wheat spikelets had no obvious effects on the activation of FgHog1 in the wild type or the *giv1* and *giv2* mutants, but the phosphorylation level of FgHog1 was slightly increased in the *giv3* mutant treated with spikelets (Supplementary Fig. 13).

**Co-immunoprecipitation assays.** The *GPA2*–GFP and $P_{RP27}$-*GIV1*–3×FLAG fusion constructs were generated by the yeast gap repair approach[46,56] and co-transformed into the wild-type strain PH-1. As *GIV1* is specifically expressed during plant infection, we used the constitutive RP27 (ribosomal protein 27) promoter[56] to express *GIV1*–3×FLAG. Conidia of the resulting transformants were inoculated in YEPD with shaking at 200 r.p.m. for 24 h. Hyphae were collected by filtration and used for protein extraction as described with 0.5% Triton X-100 in the extraction buffer to solubilize membrane-associated proteins[57]. The resulting protein supernatant was incubated with anti-FLAG M2-agarose beads (Sigma-Aldrich) and proteins that co-purified with Giv1–3×FLAG fusion were eluted as described previously[52]. Western blots of total proteins and proteins eluted from anti-FLAG M2 beads separated on 10% SDS–polyacrylamide gel electrophoresis gels were detected with the anti-GFP and anti-FLAG antibodies (Abcam) as described previously[54].

**Assays for chemotropic growth of germ tubes.** A germ tube assay has been developed for detecting chemotropic growth in *F. oxysporum*[33]. As *F. graminearum* produces multicellular ascospores and macroconidia, to use the similar chemotropic growth assay[33], we generated the *roa* mutant in PH-1 and *giv1 roa*, *giv2 roa* and *giv3 roa* mutants that produce mainly unicellular ascospores[34]. Ascospores from the resulting *roa* mutants were resuspended to $6 \times 10^4$ spores ml$^{-1}$ in DDW for chemotropic assays as described previously[33]. Briefly, ascospore suspensions were inoculated onto water agar at a central scoring line with two parallel wells (5 mm away) on both sides that were filled with 20 μl of the test compound or solvent control. After incubating at 25 °C for 6 h, the number of germ tubes with tips growing towards the test compound ($H_{test}$) or solvent ($H_{solv}$) were counted to calculate the chemotrophic index as $(H_{test} - H_{solv})/H_{total} \times 100$ (ref. [33]), in which $H_{total}$ is the total number of germ tubes examined. For each compound tested, including 1 mM of glucose, glutamine, aspartic acid, glycerol or galactose[33], data from 3 independent replicates with at least 100 germ tubes examined each were used to estimate the mean chemotrophic index. For preparing spikelet extracts, 200 mg of wheat spikelets with glumes removed and lemma pulled apart to expose floral organs were soaked in 1 ml water, chloroform, or ethyl acetate for 3 h with gentle shaking in plastic Eppendorf tubes under normal daytime laboratory conditions. After a brief spin, the supernatants were then collected and used as the test compounds in chemotropic growth assays.

**qRT–PCR assays for the expression level of six *GIV* genes.** RNA samples were isolated from hyphae of 24 h YEPD cultures and infected wheat heads sampled at 3 dpi. Relative expression levels of *GIV1*–*GIV6* genes were assayed by qRT–PCR with the ubiquitin C-terminal hydrolase gene (*GzUBH*)[58] as the internal control. Data from three biological replicates were used to estimate the mean and standard deviation.

**Assays for the PPE function in Fg07792 and *GIV5*.** The entire Fg07792 gene with its native promoter ($PPE^+$) that contains an AGACAACA sequence matching the PPE consensus was amplified and cloned into pFL2 by gap repair[38]. Overlapping PCR was used to generate a similar construct with the PPE sequence of Fg07792 deleted (ΔPPE). Both constructs were transformed into the Fg07792 deletion mutant to generate the $PPE^+$ and ΔPPE transformants. The expression level of Fg07792 in vegetative hyphae and infected wheat heads (3 dpi) was assayed by qRT–PCR. Similar approaches were used to verify the function of the PPE element (AACCGACA) in the promoter of the *GIV5* (Fg02981) gene.

**RNA-seq analysis with infected wheat heads.** For each wheat head of 6-week-old XiaoYan 22 plants, all of the florets at anthesis were drop-inoculated with 10 µl of conidium suspensions of the wild-type strain PH-1 as described previously[31]. The inoculated wheat heads were sampled at 1-, 2- and 3 dpi, and diseased spikelets were collected for RNA isolation as described previously[25]. After treatment with RNase-free DNase I, Poly(A)+mRNA was isolated with the NEBNext Poly(A) mRNA Magnetic Isolation Module (New England Biolabs) following the instructions provided by the manufacturer. Strand-specific RNA-seq libraries were constructed for 3 independent biological replicates of each time point with the NEBNext Ultra Directional RNA Library Prep Kit (New England Biolabs) and sequenced by Illumina HiSeq 2500 with the 2 × 150-base-pair paired-end read mode at Novogene Bioinformatics Technology (Beijing). The resulting RNA-seq data were deposited at NCBI SRA database under accession numbers SRR8568982–SRR8568984 and SRR8569386–SRR8569394. The RNA-seq data of vegetative hyphae and perithecia of PH-1 were generated in a previous study[25,26] and deposited in the NCBI SRA database under accession numbers SRS1044675 and SRS1044677. Low-quality reads of the RNA-seq data were removed with Trimmomatic. At least 120 million high-quality reads (Q20 > 95%; Q30 > 85%) were obtained for each time point of the infected wheat head samples and aligned to the PH-1 reference genome (V3, Broad Institute) using HISAT2 with its two-step algorithm. The number of reads (counts) aligned to each gene was calculated by FeatureCounts. Gene expression counts were normalized using the TPM method[59].

**Statistics and reproducibility statement.** The qPCR data from 3 independent replicates were analysed for statistical differences with Bootstrap analysis by BootstRatio[60] ($P = 0.0005$). For disease indices scored with infected wheat heads, lesion lengths on wheat seedlings, PKA activities, TpEY assays, chemotropic indices of germ tubes, intracellular cAMP concentrations and localization of Gpmk1–GFP to the nucleus, statistical analyses were performed with data from at least three independent biological replicates using one-sided ANOVA analysis followed by Duncan's multiple range test ($P = 0.05$). Assays with growth rate, conidiation and perithecium formation were repeated five independent times with all of the mutant strains. For assaying infection cushion formation and colonization of flowering wheat heads, three independent experiments were repeated with the wheat cultivar XiaoYan 22 (ref. [48]). Six independent experiments were conducted with three-day-old seedlings to assay infectious growth in wheat coleoptile cells.

**Reporting Summary.** Further information on research design is available in the Nature Research Reporting Summary linked to this article.

## Data availability

The data that support the findings of this study are available from the corresponding author and C. J. (cjiang@nwafu.edu.cn) upon request. RNA-seq data generated in this study are accessible under the accession numbers SRR8568982–SRR8568984 and SRR8569386–SRR8569394.

Received: 7 August 2018; Accepted: 25 April 2019;
Published online: 03 June 2019

## References

1. Goswami, R. S. & Kistler, H. C. Heading for disaster: *Fusarium graminearum* on cereal crops. *Mol. Plant Pathol.* **5**, 515–525 (2004).
2. Brown, N. A., Urban, M., Van De Meene, A. M. L. & Hammond-Kosack, K. E. The infection biology of *Fusarium graminearum*: Defining the pathways of spikelet to spikelet colonisation in wheat ears. *Fungal Biol.* **114**, 555–571 (2010).
3. Bai, G. H. & Shaner, G. Management and resistance in wheat and barley to *Fusarium* head blight. *Annu. Rev. Phytopathol.* **42**, 135–161 (2004).
4. Strange, R., Majer, J. & Smith, H. The isolation and identification of choline and betaine as the two major components in anthers and wheat germ that stimulate *Fusarium graminearum* in vitro. *Physiol. Plant Pathol.* **4**, 277–290 (1974).
5. Urban, M., Daniels, S., Mott, E. & Hammond-Kosack, K. *Arabidopsis* is susceptible to the cereal ear blight fungal pathogens *Fusarium graminearum* and *Fusarium culmorum*. *Plant J.* **32**, 961–973 (2002).
6. Jiang, C., Zhang, X., Liu, H. Q. & Xu, J. R. Mitogen-activated protein kinase signaling in plant pathogenic fungi. *PLoS Pathol.* **14**, e1006875 (2018).
7. Jenczmionka, N. J., Maier, F. J., Losch, A. P. & Schafer, W. Mating, conidiation and pathogenicity of *Fusarium graminearum*, the main causal agent of the head-blight disease of wheat, are regulated by the MAP kinase Gpmk1. *Curr. Genet.* **43**, 87–95 (2003).
8. Cuzick, A., Urban, M. & Hammond-Kosack, K. *Fusarium graminearum* gene deletion mutants *map1* and *tri5* reveal similarities and differences in the pathogenicity requirements to cause disease on *Arabidopsis* and wheat floral tissue. *New Phytol.* **177**, 990–1000 (2008).
9. Hu, S. et al. The cAMP–PKA pathway regulates growth, sexual and asexual differentiation, and pathogenesis in *Fusarium graminearum*. *Mol. Plant Microbe Interact.* **27**, 557–566 (2014).
10. Bormann, J., Boenisch, M. J., Bruckner, E., Firat, D. & Schafer, W. The adenylyl cyclase plays a regulatory role in the morphogenetic switch from vegetative to pathogenic lifestyle of *Fusarium graminearum* on wheat. *PLoS ONE* **9**, e91135 (2014).
11. Nguyen, T. V., Schafer, W. & Bormann, J. The stress-activated protein kinase FgOS-2 is a key regulator in the life cycle of the cereal pathogen *Fusarium graminearum*. *Mol. Plant Microbe Interact.* **25**, 1142–1156 (2012).
12. Hou, Z. M. et al. A mitogen-activated protein kinase gene (*MGV1*) in *Fusarium graminearum* is required for female fertility, heterokaryon formation, and plant infection. *Mol. Plant Microbe Interact.* **15**, 1119–1127 (2002).
13. Li, L., Wright, S. J., Krystofova, S., Park, G. & Borkovich, K. A. Heterotrimeric G protein signaling in filamentous fungi. *Annu. Rev. Microbiol.* **61**, 423–452 (2007).
14. Yu, H. Y. et al. Functional analyses of heterotrimeric G protein G alpha and G beta subunits in *Gibberella zeae*. *Microbiology* **154**, 392–401 (2008).
15. Cabrera, I. E. et al. Global analysis of predicted G protein-coupled receptor genes in the filamentous fungus, *Neurospora crassa*. *Genes Genom. Genet.* **5**, 2729–2743 (2015).
16. Bieszke, J. A. et al. The *nop-1* gene of *Neurospora crassa* encodes a seven transmembrane helix retinal-binding protein homologous to archaeal rhodopsins. *Proc. Natl Acad. Sci. USA* **96**, 8034–8039 (1999).
17. DeZwaan, T. M., Carroll, A. M., Valent, B. & Sweigard, J. A. *Magnaporthe grisea* Pth11p is a novel plasma membrane protein that mediates appressorium differentiation in response to inductive substrate cues. *Plant Cell* **11**, 2013–2030 (1999).
18. Kou, Y., Tan, Y. H., Ramanujam, R. & Naqvi, N. I. Structure-function analyses of the Pth11 receptor reveal an important role for CFEM motif and redox regulation in rice blast. *New Phytol.* **214**, 330–342 (2017).
19. Lee, J. K., Leslie, J. F. & Bowden, R. L. Expression and function of sex pheromones and receptors in the homothallic ascomycete *Gibberella zeae*. *Eukaryot. Cell* **7**, 1211–1221 (2008).
20. Ma, L. J. et al. Comparative genomics reveals mobile pathogenicity chromosomes in Fusarium. *Nature* **464**, 367–373 (2010).
21. Cuomo, C. A. et al. The *Fusarium graminearum* genome reveals a link between localized polymorphism and pathogen specialization. *Science* **317**, 1400–1402 (2007).
22. Brown, N. A., Schrevens, S., van Dijck, P. & Goldman, G. H. Fungal G-protein-coupled receptors: mediators of pathogenesis and targets for disease control. *Nat. Microbiol.* **3**, 402–414 (2018).
23. Tucker, S. L. et al. Common genetic pathways regulate organ-specific infection-related development in the rice blast fungus. *Plant Cell* **22**, 953–972 (2010).
24. Li, L. & Borkovich, K. A. GPR-4 is a predicted G-protein-coupled receptor required for carbon source-dependent asexual growth and development in *Neurospora crassa*. *Eukaryot. Cell* **5**, 1287–1300 (2006).
25. Liu, H. Q. et al. Genome-wide A-to-I RNA editing in fungi independent of ADAR enzymes. *Genome Res.* **26**, 499–509 (2016).
26. Chen, D. P. et al. Sexual specific functions of Tub1 beta-tubulins require stage-specific RNA processing and expression in *Fusarium graminearum*. *Environ. Microbiol.* **20**, 4009–4021 (2018).
27. Boenisch, M. J. & Schafer, W. *Fusarium graminearum* forms mycotoxin producing infection structures on wheat. *BMC Plant Biol.* **11**, 110 (2011).
28. Becker, M., Becker, Y., Green, K. & Scott, B. The endophytic symbiont *Epichloe festucae* establishes an epiphyllous net on the surface of *Lolium perenne* leaves by development of an expressorium, an appressorium-like leaf exit structure. *New Phytol.* **211**, 240–254 (2016).
29. Park, A. R. et al. Functional analyses of regulators of G protein signaling in *Gibberella zeae*. *Fungal Genet. Biol.* **49**, 511–520 (2012).
30. Miller, S. S., Chabot, D. M. P., Ouellet, T., Harris, L. J. & Fedak, G. Use of a *Fusarium graminearum* strain transformed with green fluorescent protein to study infection in wheat (*Triticum aestivum*). *Can. J. Plant Pathol.* **26**, 453–463 (2004).

31. Zhang, X. W. et al. In planta stage-specific fungal gene profiling elucidates the molecular strategies of *Fusarium graminearum* growing inside wheat coleoptiles. *Plant Cell* **24**, 5159–5176 (2012).
32. Ma, L. S. et al. The *Ustilago maydis* repetitive effector Rsp3 blocks the antifungal activity of mannose-binding maize proteins. *Nat. Commun.* **9**, 1711 (2018).
33. Turra, D., El Ghalid, M., Rossi, F. & Di Pietro, A. Fungal pathogen uses sex pheromone receptor for chemotropic sensing of host plant signals. *Nature* **527**, 521 (2015).
34. Min, K. et al. A novel gene, *ROA*, is required for normal morphogenesis and discharge of ascospores in *Gibberella zeae*. *Eukaryot. Cell* **9**, 1495–1503 (2010).
35. Jiang, C. et al. *TRI6* and *TRI10* play different roles in the regulation of deoxynivalenol (DON) production by cAMP signalling in *Fusarium graminearum*. *Environ. Microbiol.* **18**, 3689–3701 (2016).
36. Zhao, X. H., Kim, Y., Park, G. & Xu, J. R. A mitogen-activated protein kinase cascade regulating infection-related morphogenesis in *Magnaporthe grisea*. *Plant Cell* **17**, 1317–1329 (2005).
37. Wang, C. F. et al. Functional analysis of the kinome of the wheat scab fungus Fusarium graminearum. *PLoS Pathol.* **7**, e1002460 (2011).
38. Bruno, K. S., Tenjo, F., Li, L., Hamer, J. E. & Xu, J. R. Cellular localization and role of kinase activity of PMK1 in *Magnaporthe grisea*. *Eukaryot. Cell* **3**, 1525–1532 (2004).
39. Raviv, Z., Kalie, E. & Seger, R. MEK5 and ERK5 are localized in the nuclei of resting as well as stimulated cells, while MEKK2 translocates from the cytosol to the nucleus upon stimulation. *J. Cell Sci.* **117**, 1773–1784 (2004).
40. Wang, Q. et al. Characterization of the two-speed subgenomes of *Fusarium graminearum* reveals the fast-speed subgenome specialized for adaption and infection. *Front. Plant Sci.* **8**, 140 (2017).
41. Son, H. et al. A phenome-based functional analysis of transcription factors in the cereal head blight fungus, *Fusarium graminearum*. *PLoS Pathol.* **7**, e1002310 (2011).
42. Kulkarni, R. D., Thon, M. R., Pan, H. Q. & Dean, R. A. Novel G-protein-coupled receptor-like proteins in the plant pathogenic fungus *Magnaporthe grisea*. *Genome Biol.* **6**, 24 (2005).
43. Li, G. T., Zhou, X. Y. & Xu, J. R. Genetic control of infection-related development in *Magnaporthe oryzae*. *Curr. Opin. Microbiol.* **15**, 678–684 (2012).
44. Sakulkoo, W. et al. A single fungal MAP kinase controls plant cell-to-cell invasion by the rice blast fungus. *Science* **359**, 1399 (2018).
45. Zhang, X., Liu, W. D., Li, Y., Li, G. T. & Xu, J. R. Expression of HopAI interferes with MAP kinase signalling in *Magnaporthe oryzae*. *Environ. Microbiol.* **19**, 4190–4204 (2017).
46. Zhou, X., Li, G. & Xu, J. R. Efficient approaches for generating GFP fusion and epitope-tagging constructs in filamentous fungi. *Methods Mol. Biol.* **722**, 199–212 (2011).
47. Madhani, H. D., Styles, C. A. & Fink, G. R. MAP kinases with distinct inhibitory functions impart signaling specificity during yeast differentiation. *Cell* **91**, 673–684 (1997).
48. Kang, Z. S., Buchenauer, H., Huang, L. L., Han, Q. M. & Zhang, H. C. Cytological and immunocytochemical studies on responses of wheat spikes of the resistant Chinese cv. Sumai 3 and the susceptible cv. Xiaoyan 22 to infection by *Fusarium graminearum*. *Eur. J. Plant Pathol.* **120**, 383–396 (2008).
49. Chen, X. H., Zhang, L., Zhao, J. X., Wu, J. & Liu, S. H. Study and utilize on a new wheat variety of nation approve Xiaoyan22. *Chin. Agri. Sci. Bull.* **9**, 218–220 (2007).
50. Jonkers, W., Dong, Y. H., Broz, K. & Kistler, H. C. The Wor1-like protein Fgp1 regulates pathogenicity, toxin synthesis and reproduction in the phytopathogenic fungus *Fusarium graminearum*. *PLoS Pathol.* **8**, e1002724 (2012).
51. Ding, S. L. et al. Transducin beta-like gene *FTL1* Is essential for pathogenesis in *Fusarium graminearum*. *Eukaryot. Cell* **8**, 867–876 (2009).
52. Yin, T. et al. The cyclase-associated protein FgCap1 has both protein kinase A-dependent and -independent functions during deoxynivalenol production and plant infection in *Fusarium graminearum*. *Mol. Plant Pathol.* **19**, 552–563 (2018).
53. Ramanujam, R. & Naqvi, N. I. PdeH, a high-affinity cAMP phosphodiesterase, is a key regulator of asexual and pathogenic differentiation in *Magnaporthe oryzae*. *PLoS Pathol.* **6**, e1000897 (2010).
54. Zhang, X., Bian, Z. & Xu, J. R. in *Plant Pathogenic Fungi and Oomycetes* (eds Ma, W. B. & Wolpert, T.) Ch. 8 (Springer, 2018).
55. Zheng, D. W. et al. The FgHOG1 pathway regulates hyphal growth, stress responses, and plant infection in *Fusarium graminearum*. *PLoS ONE* **7**, e49495 (2012).
56. Ding, S. L. et al. The Tig1 histone deacetylase complex regulates infectious growth in the rice blast fungus *Magnaporthe oryzae*. *Plant Cell* **22**, 2495–2508 (2010).
57. Krystofova, S. & Borkovich, K. A. The heterotrimeric G-protein subunits GNG-1 and GNB-1 form a Gbetagamma dimer required for normal female fertility, asexual development, and galpha protein levels in *Neurospora crassa*. *Eukaryot. Cell* **4**, 365–378 (2005).
58. Kim, H. K. & Yun, S. H. Evaluation of potential reference genes for quantitative RT-PCR analysis in *Fusarium graminearum* under different culture conditions. *Plant Pathol. J.* **27**, 301–309 (2011).
59. Wagner, G. P., Kin, K. & Lynch, V. J. Measurement of mRNA abundance using RNA-seq data: RPKM measure is inconsistent among samples. *Theor. Biosci.* **131**, 281–285 (2012).
60. Cleries, R. et al. BootstRatio: A web-based statistical analysis of fold-change in qPCR and RT-qPCR data using resampling methods. *Comput. Biol. Med.* **42**, 438–445 (2012).


## Acknowledgements

We thank W. Wang, R. Hei, H. Jiang, J. Ren, P. Huang, C. Wu and C. Wang for assistance with generating GPCR gene deletion mutants. We also thank L. Dunkle and P. Goldsbrough at Purdue University for critical reading of this manuscript. This work was supported by grants from the National Natural Science Foundation of China (no. 31772114), NSWBSI, USDA NIFA (Award no. 2013-68004-20378), Tang Scholar and the Natural Science Basic Research Plan in Shaanxi Province of China (no. 2017JM3001).

## Author contributions

J.-R.X. and C.J. designed the research and wrote the paper. C.J., S.C., Z.W., H.X., J.L., G.W., M.D., C.G., C.F. and C.H. performed the experiments. C.J., H.L. and Q.W. analysed the data.

## Competing interests

The authors declare no competing interests.

## Additional information

**Supplementary information** is available for this paper at https://doi.org/10.1038/s41564-019-0468-8.

**Reprints and permissions information** is available at www.nature.com/reprints.

**Correspondence and requests for materials** should be addressed to J.-R.X.

**Publisher's note:** Springer Nature remains neutral with regard to jurisdictional claims in published maps and institutional affiliations.

nature research

Corresponding author(s): Jin-Rong Xu

Last updated by author(s): Apr 16, 2019

# Reporting Summary

Nature Research wishes to improve the reproducibility of the work that we publish. This form provides structure for consistency and transparency in reporting. For further information on Nature Research policies, see Authors & Referees and the Editorial Policy Checklist.

## Statistics

For all statistical analyses, confirm that the following items are present in the figure legend, table legend, main text, or Methods section.

| n/a | Confirmed | |
|---|---|---|
| ☐ | ☒ | The exact sample size (*n*) for each experimental group/condition, given as a discrete number and unit of measurement |
| ☐ | ☒ | A statement on whether measurements were taken from distinct samples or whether the same sample was measured repeatedly |
| ☐ | ☒ | The statistical test(s) used AND whether they are one- or two-sided<br>*Only common tests should be described solely by name; describe more complex techniques in the Methods section.* |
| ☒ | ☐ | A description of all covariates tested |
| ☒ | ☐ | A description of any assumptions or corrections, such as tests of normality and adjustment for multiple comparisons |
| ☐ | ☒ | A full description of the statistical parameters including central tendency (e.g. means) or other basic estimates (e.g. regression coefficient) AND variation (e.g. standard deviation) or associated estimates of uncertainty (e.g. confidence intervals) |
| ☐ | ☒ | For null hypothesis testing, the test statistic (e.g. *F*, *t*, *r*) with confidence intervals, effect sizes, degrees of freedom and *P* value noted<br>*Give P values as exact values whenever suitable.* |
| ☒ | ☐ | For Bayesian analysis, information on the choice of priors and Markov chain Monte Carlo settings |
| ☒ | ☐ | For hierarchical and complex designs, identification of the appropriate level for tests and full reporting of outcomes |
| ☒ | ☐ | Estimates of effect sizes (e.g. Cohen's *d*, Pearson's *r*), indicating how they were calculated |

*Our web collection on statistics for biologists contains articles on many of the points above.*

## Software and code

Policy information about availability of computer code

| | |
|---|---|
| Data collection | Bio-Rad CFX manager for qPCR data collection and analysis. |
| Data analysis | Band densities were analyzed with the Image Lab™ software. SPSS Statistics for statistical analysis. Multiple sequence alignments were generated with the M-Coffee program. Phylogenetic trees were constructed with the Neighbor-Joining method using MEGA and further edited using the ITOL tool. Heat maps were constructed with the gplot package in R with published RNA-seq data. The 1 kb sequences upstream from the transcription initiation site of all the GPCR genes were analyzed by the MEME Suite for common promoter elements. Transmembrane (TM) helices were predicted by TMHMM 2.0 and TOPCONS. |

For manuscripts utilizing custom algorithms or software that are central to the research but not yet described in published literature, software must be made available to editors/reviewers. We strongly encourage code deposition in a community repository (e.g. GitHub). See the Nature Research guidelines for submitting code & software for further information.

## Data

Policy information about availability of data

All manuscripts must include a data availability statement. This statement should provide the following information, where applicable:

- Accession codes, unique identifiers, or web links for publicly available datasets
- A list of figures that have associated raw data
- A description of any restrictions on data availability

*Provide your data availability statement here.*

# Field-specific reporting

Please select the one below that is the best fit for your research. If you are not sure, read the appropriate sections before making your selection.

☒ Life sciences ☐ Behavioural & social sciences ☐ Ecological, evolutionary & environmental sciences

For a reference copy of the document with all sections, see nature.com/documents/nr-reporting-summary-flat.pdf

# Life sciences study design

All studies must disclose on these points even when the disclosure is negative.

| | |
|---|---|
| Sample size | When assays for disease index, mean and standard deviation of the disease index of each strain were estimated with data from three (n=3) independent experiments (marked with black dots on the bars) with at least 10 biological replicates (n≥10 infected wheat heads) examined for each experiment. When assays for infection cushions formation, Mean and standard deviation were estimated with data from three (n=3) independent experiments (marked with black dots on the bars) with four biological replicates (n=4 inoculated wheat lemma) examined for each replicate. When assays for chemotropic index, three (n=3) individual biological replicates were performed with 100 germ tubes examined in each replicate. When assays for the effects of wheat spikelets on PKA activities and activation of MAP kinases, mean and standard deviation of the ratio between treated and untreated samples were estimated with data from three (n=3) independent replicates. When assays for the Gpmk1 localization, Mean and standard deviation of the percentage of type A nuclei were estimated with data from three (n=3) independent replicates. For each replicate, 60 germ tubes were examined (n=60). Three (n=3) independent biological replicates for qPCR assays. No statistical methods were used to predetermine sample sizes. These sample sizes are commonly used in Fusarium graminearum studies and sufficient for statistical analyses. |
| Data exclusions | No data were excluded from the analyses |
| Replication | All attempts at replication were successful. The number of replicates is indicated in the corresponding figure legend and/or in the corresponding material and method section. |
| Randomization | Randomization was used for all the biological experiments. |
| Blinding | No blinding was done as none of the experiments described in this study involve group allocation during data collection or analyses. |

# Reporting for specific materials, systems and methods

We require information from authors about some types of materials, experimental systems and methods used in many studies. Here, indicate whether each material, system or method listed is relevant to your study. If you are not sure if a list item applies to your research, read the appropriate section before selecting a response.

## Materials & experimental systems

| n/a | Involved in the study |
|---|---|
| ☐ | ☒ Antibodies |
| ☐ | ☒ Eukaryotic cell lines |
| ☒ | ☐ Palaeontology |
| ☐ | ☒ Animals and other organisms |
| ☒ | ☐ Human research participants |
| ☒ | ☐ Clinical data |

## Methods

| n/a | Involved in the study |
|---|---|
| ☒ | ☐ ChIP-seq |
| ☒ | ☐ Flow cytometry |
| ☒ | ☐ MRI-based neuroimaging |

## Antibodies

| | |
|---|---|
| Antibodies used | PhophoPlus p44/42 MAP kinase antibody (Cat. #4370, Cell Signaling Technology, USA, Dilution 1:1000), Phopho p38 MAP kinase antibody (Cat. #4511, Cell Signaling Technology, Dilution 1:1000), Anti-Erk2 antibody (Cat. #Sc-1271451, Santa Cruz Biotechnology, USA, Dilution 1:1000), Anti-H3 antibody (ab209023, Abcam, UK, Dilution 1:1000), Anti-GFP antibody (Cat. #11814460001, Roche, Switzerland, Dilution 1:1000), Anti-FLAG antibody (F3165, Sigma-Aldrich, USA, Dilution 1:1000). |
| Validation | All the primary antibodies used in this study have been published in earlier studies in Fusarium graminearum, including the anti-Erk2, anti-p38, anti-TpEY, and anti-TpGY antibodies that were further validated with the gpmk1, mgv1, and Fghog1 deletion mutants in this study (Supplementary Figure 22). |

## Eukaryotic cell lines

Policy information about cell lines

| | |
|---|---|
| Cell line source(s) | *State the source of each cell line used.* |

| | |
|---|---|
| Authentication | *Describe the authentication procedures for each cell line used OR declare that none of the cell lines used were authenticated.* |
| Mycoplasma contamination | *Confirm that all cell lines tested negative for mycoplasma contamination OR describe the results of the testing for mycoplasma contamination OR declare that the cell lines were not tested for mycoplasma contamination.* |
| Commonly misidentified lines (See ICLAC register) | *Name any commonly misidentified cell lines used in the study and provide a rationale for their use.* |

## Animals and other organisms

Policy information about studies involving animals; ARRIVE guidelines recommended for reporting animal research

| | |
|---|---|
| Laboratory animals | This study did not involved laboratory animals. Fusarium graminearum (plant pathogenic fungus) is involved. |
| Wild animals | *Provide details on animals observed in or captured in the field; report species, sex and age where possible. Describe how animals were caught and transported and what happened to captive animals after the study (if killed, explain why and describe method; if released, say where and when) OR state that the study did not involve wild animals.* |
| Field-collected samples | *For laboratory work with field-collected samples, describe all relevant parameters such as housing, maintenance, temperature, photoperiod and end-of-experiment protocol OR state that the study did not involve samples collected from the field.* |
| Ethics oversight | *Identify the organization(s) that approved or provided guidance on the study protocol, OR state that no ethical approval or guidance was required and explain why not.* |

Note that full information on the approval of the study protocol must also be provided in the manuscript.